THE ASTROPHYSICAL JOURNAL, 325:402–410, 1988 February 1

HIGH-RESOLUTION SOUNDING ROCKET OBSERVATIONS OF INTERSTELLAR H_2 LINES TOWARD δ SCORPII

THEODORE P. SNOW, WILLIAM E. MCCLINTOCK, AND STEPHEN A. VOELS
Center for Astrophysics and Space Astronomy and Laboratory for Atmospheric and Space Physics, University of Colorado, Boulder
Received 1987 January 19; accepted 1987 July 16

ABSTRACT

We report the results of observations made with our far-ultraviolet echelle spectrograph launched in 1984 July on a sounding rocket. The instrument recorded interstellar absorption lines from the Lyman system of H_2 at a resolving power $\lambda/\Delta\lambda = 60{,}000$ toward the B0.5 IV star δ Sco. From equivalent widths we derived a total H_2 column density of 2.8×10^{19} cm^{-2} and inferred a kinetic temperature of 62 K from the population ratio of the $J = 0$ and $J = 1$ rotational states. Our excitation temperature of 210 K for J levels between 2 and 5 gives constraints on the H_2 formation rate and the cloud volume density, and it implies that the local ultraviolet radiation field is roughly 6 times as intense as the average value in the solar neighborhood.

We were able to measure relative line velocities to an accuracy of ± 3 km s^{-1}. We found no systematic velocity separation between lines arising from different rotational levels, implying that the high-J lines are not formed in an expanding circumstellar bubble, as had been suggested by an earlier investigation of H_2 lines toward other stars at lower resolution. Our data quality was not sufficient to measure the widths of absorption-line profiles.

Subject headings: interstellar: abundances — interstellar: molecules — stars: individual (δ Sco) — ultraviolet: spectra

I. INTRODUCTION

Ultraviolet spectroscopy of interstellar absorption lines has proved to be a powerful tool for analyzing the composition and physical state of the diffuse interstellar medium. Early rocket data (e.g., Carruthers 1970; Jenkins 1973) and especially the Copernicus satellite (e.g., Morton *et al.* 1973; Spitzer and Jenkins 1975) have revolutionized our knowledge in this field. Today the *International Ultraviolet Explorer* (*IUE*) satellite is producing useful interstellar gas data, and we are all anticipating the major advances expected with the Hubble Space Telescope.

To date, however, ultraviolet data have not been available with spectral resolution comparable to the best obtained with ground-based instrumentation, where resolving powers ($R = \lambda/\Delta\lambda$) as high as 10^5–10^6 have been achieved (e.g., Hobbs 1978 and references cited therein; Blades, Wynn-Jones, and Wayte 1980). The very high resolution ground-based data show, however, that enormous benefits are gained, even in a spectral region where there are few interstellar lines representing only trace elements. It is clear that even greater gains will be possible when comparable resolutions are achieved in the ultraviolet. This paper reports the results of the first observations made with a new rocket-borne ultraviolet echelle spectrograph having a resolving power ($R = 60{,}000$) significantly greater than previously achieved (except with the Balloon-borne Ultraviolet Stellar Spectrograph [BUSS] payload which was recently flown by a Dutch group, and which has comparable resolution; we note also that another rocket-borne instrument with $R = 100{,}000$ was recently flown by E. B. Jenkins). This is a factor of 3 better resolution than *Copernicus*, corresponding to a velocity resolution of about 5 km s^{-1} in the far-ultraviolet.

The scientific problem that motivated the research described here is the study of rotational excitation in H_2 molecules. *Copernicus* data showed that in diffuse clouds the rotational excitation of H_2 generally reflected at least two different physical mechanisms: the $J = 0$ and $J = 1$ populations appeared to be in thermal equilibrium with the gas, while the higher rotational levels appeared to represent a higher rotational temperature, indicating that some nonthermal process is at work. It was suggested that the excitation of the high J levels might reflect the initial energy given to newly formed molecules as they escaped from grain surfaces (Spitzer and Zweibel 1974), but eventually it became accepted that the dominant mechanism is ultraviolet pumping (Black and Dalgarno 1976; Jura 1975*a*, *b*; Shull and Beckwith 1983). This refers to the fact that when an H_2 molecule absorbs an ultraviolet photon in one of the Lyman or Werner bands and thus becomes electronically excited, it will cascade through a series of excited vibrational and rotational levels of the ground electronic state as it relaxes. Because the spontaneous emission probabilities for the downward transitions in the cascade are finite, there is an equilibrium fraction of molecules in excited rotational levels of the ground state. This accounts for the relatively high populations observed in the $J > 2$ levels of H_2, and allows important information on cloud densities and ultraviolet radiation field intensities to be derived from the observed rotational excitation. That is part of the intent of the research described here.

Another manifestation of the population of high rotational levels was possibly observed by Spitzer and Morton (1976). Using *Copernicus* data, with its 15 km s^{-1} resolution, Spitzer and Morton found a tendency for the lines arising from high J levels to be shifted toward shorter wavelengths (more negative velocity) than the $J = 0$ and $J = 1$ lines, as though the material in which the excited lines arise were systematically moving toward us, relative to the material where the low-excitation lines are formed. The high-J lines were also found to be systematically broader than those arising from low rotational states.

A possible explanation offered by Spitzer and Morton was that the highly excited lines arise in material being ejected by the O and B stars used as background continuum sources. Thus, the excited H_2 would exist primarily in gas that is relatively close to the star, where the intense local ultraviolet radiation field would provide the pumping. This picture is at least qualitatively consistent with the theoretical prediction that O and B stars with strong winds should create circumstellar "bubbles" due to swept-up material (Castor, McCray, and Weaver 1975; Weaver *et al.* 1977). The swept-up gas would reach a steady velocity of the order of 10–15 km s^{-1} relative to the star, and this is comparable to the apparent velocity shift observed by Spitzer and Morton (1976). It is also reasonable to expect that the swept-up gas would have a high internal velocity dispersion, accounting for the greater line widths of the highest lines. Unfortunately, the expected bubble expansion velocity is comparable to the velocity resolution of *Copernicus*, so it was difficult to pursue the question of possible velocity separation of the high-J lines any further. The velocity resolution of our instrument, however, is adequate for the job, and testing the hypothesis that the excited lines are shifted was part of the goal of the present research.

The instrument and the observations are described in the next section, followed by a description of the data characteristics and reduction (§ III). The results of the abundance analysis for the first six rotational levels are reported in § IV, and the implications are discussed in § V. Section VI summarizes the results.

II. THE INSTRUMENT AND THE OBSERVATIONS

a) *Instrument Description*

The instrument consists of a Cassegrain telescope and echelle spectrograph, designed and built in the Laboratory for Atmospheric and Space Physics at the University of Colorado, coupled to a coincidence anode microchannel plate photon detector (Multi-Anode Microchannel Array [MAMA] detector) designed and built at Ball Aerospace Systems. In order to achieve a resolution $\lambda/\Delta\lambda = 60{,}000$, the telescope secondary mirror is servocontrolled to correct for tracking errors and jitter in the rocket attitude-control system, providing ultimate stellar image stabilization and positioning of 1″ in the telescope focal plane. The spectrograph is a modified Czerny-Turner design in which the spherical camera mirror was replaced by a concave grating used in a Wadsworth mount. For the observations described here, the spectrograph was aligned so that 7 echelle orders ($N = 127$ to $N = 134$) centered at 1075 Å were incident on the detector. Design parameters for the instrument optics are summarized in Table 1.

The spectrograph detector consists of a curved microchannel plate output to a two-dimensional pulse-counting anode array which has 24 rows of 1024 pixels. Each pixel is 0.025 mm wide by 0.260 mm high. Readout of the detector is accomplished photon by photon in a technique described by Timothy and Bybee (1981).

b) *Observations*

The primary target star chosen for the H_2 study was δ Sco [B0.5 IV; $V = 2.33$; $E(B-V) = 0.16$]. This object was chosen because it is extremely bright in the ultraviolet (about 10 times brighter than the well-studied ζ Ophiuchi), and because it lies in the ρ Ophiuchi cloud, a region with very interesting properties (such as low ultraviolet extinction, high overall density, and high depletions [see Carrasco, Strom, and Strom 1973]; for the ρ Oph cloud see Snow and Jenkins 1980 and other papers cited below). Some H_2 data are already available from earlier *Copernicus* observations. Overall column densities were derived for several stars from the $J = 0$ and $J = 1$ lines by Bohlin, Savage, and Drake (1978), and δ Sco was included in the survey of H_2 excitation by Spitzer, Cochran, and Hirshfeld (1974). In addition, rotational excitation toward σ Sco was analyzed by Snow (1983*a*; this is discussed in § V, below). Several other ρ Oph cloud stars are bright enough for detailed *Copernicus* observations of H_2 rotational lines, but none were made.

Another interesting aspect of the ρ Oph cloud region is that there is some evidence for velocity structure in interstellar lines (Hobbs 1978; Meyers *et al.* 1985). Although δ Sco itself does not have a strong wind (Snow and Morton 1976), it does have a high-velocity outflow (Snow 1981), but the wind density is apparently lower than for other stars of similar luminosity and spectral class. Hence, it was not clear initially whether to expect this star to have a well-developed circumstellar bubble.

The instrument was launched from White Sands Missile Range aboard a Nike Black Brant rocket on 1984 June 24 at 6:14 UT. The primary target, δ Sco, was observed for 206 s. In order to realize the full resolution of a detector with 0.025 mm pixels on 0.025 mm centers, it was necessary to obtain two independent spectra of the target star, each separated by a half-integral number of pixels. This was accomplished by using two separate entrance slits which had center-to-center separations of 0.0875 mm (3.5 pixels). During the flight, the stellar image was projected down one entrance slit for half the observing time and then down the second slit using a slit jaw television camera to monitor the telescope focal plane and real-time ground commands sent to the telescope secondary mirror control system.

On the down leg of the flight α Virginis [B1 III–IV, $V = 0.98$, $E(B-V) = 0.03$] was observed for 74 s in order to calibrate the fixed-pattern noise due to the pixel-to-pixel sensitivity variations in the spectrograph detector (discussed below).

TABLE 1

INSTRUMENT SUMMARY

Instrument and Parameters	Value
Cassegrain telescope:	
Aperture	400 mm
Focal length	6000 mm
Focal-plane scale	0.029 mm $arcsec^{-1}$
Echelle-Wadsworth spectrograph:	
Focal length	750 mm
Entrance slit	0.025 × 0.10 mm
Echelle ruling	101.95 G mm^{-1}
Echelle blaze angle	45°
Cross disperser ruling	1600 g mm^{-1}
Cross disperser blaze angle	4°.6
Wavelength range	1050–1100 Å
Multianode microchannel array detector:	
Anode	Coincidence anode
Format	24 × 1024
Pixel size	0.025 × 0.260 mm
Photocathode	Cesium iodide

III. DATA CHARACTERISTICS AND TREATMENT

a) *Conversion of Raw Data to Scientific Form*

The detector was operated in continuous readout mode during flight. The readout time is approximately 3.75 s for the entire electronics system. This gives an effective integration time of 3.75 s per pixel per readout. From the attitude telemetry and the event counter, it was determined which readouts belonged to which data set. The appropriate 3.75 s integrations were co-added to form three working data sets (δ Sco, slits 1 and 2, and α Vir). In each set, the data were kept in the form of counts per pixel along the 24 rows of the detector format. Because the spectral orders were tilted by about 3°, each spectral order traversed parts of five detector rows. The reduction was carried through to the point where all instrumental signatures had been removed before the spectral orders were extracted.

Because there was a large scattered-light contribution to the data, it was not appropriate to simply divide the δ Sco data by the α Vir data to remove the fixed-pattern noise and normalize the data. Instead a more complicated method using fast Fourier transforms (FFTs) to create a flat field and remove background was used.

A flat-field data set to remove the high-frequency pixel-to-pixel variations was created using the α Vir data set (low-frequency variations are not needed because we planned to normalize the data). This was done by applying a FFT to each row of the α Vir data set, then truncating the FFT in frequency space, so as to eliminate high-frequency variations in the retransformed data. The original α Vir data set was then divided by this retransformed data to form a flat field normalized to unity. This method introduced spurious oscillations near the ends of each row (30 pixels), but since the ends were not used because of low signal, this did not affect the final analysis.

After the two δ Sco data sets were divided by the flat field, the scattered-light correction was determined by an empirical technique. It was assumed that the general form of the background was the same for each row, so that this form could be derived from the pieces of rows where the separation of spectral orders was the greatest and the shape of the scattered light appeared cleanest. The resultant pieces were combined and smoothed by FFTs, truncating to remove high-frequency contributions. This scattered-light function was than scaled by eye and applied individually to each row of the two δ Sco data sets.

Next, the spectral orders were extracted by simply adding together the segments of each detector row that intersected each spectral order. This had the effect of compressing each order into a one-dimensional array of counts versus pixel number, which could then be wavelength-calibrated.

Finally, the two δ Sco spectra were combined, first shifting the second with respect to the first by 3.5 pixels, compensating for the projected separation of the two slits in the detector plane.

b) *Photometric Quality*

In principle the MAMA detector is photon-noise limited but in practice there were additional sources of noise, at least in certain situations, in the detector used in this payload. One is due to the variable sensitivity from pixel to pixel, which results in a "fixed-pattern" noise contribution, already discussed. After division of the target star data by the comparison data (described above), there was a substantial reduction of the fixed-pattern noise in many wavelength regions, but not uniformly throughout the spectrum. In some places, there remained a regular pattern of extreme noise excursions (Fig. 1). We believe that this pattern results from imperfect removal of the fixed pattern, most likely because of "beats" between the spacing of the anode wires and the channels in the microchannel plate of the detector, which were comparable in size. Thus, the noise peaks are effectively due to a moiré pattern.

Where the regular series of noise spikes did not occur, the random noise remaining in the data is consistent with that expected from photon statistics. Because the residual fixed-pattern noise is periodic, and affects only single pixels, it was easy to disregard this noise in measuring the equivalent widths of absorption lines that were many pixels wide.

The noise due to cosmic rays striking the detector is negligible (for the duration of a sounding rocket flight), as are any sources of noise due to thermal effects. Thus, the dominant form of random noise is due to photon statistics.

Apart from random noise, however, another, probably more serious, contribution to uncertainty in equivalent width measurements results from uncertainty in the scattered-light level. This arises primarily from the difficulty in assessing the scattered light in the spectrograph. We estimated the scattered-light background as described in the previous section, but it was clear that some residual scattered light remained, because after correction the count rates were still above zero at the centers of saturated absorption lines. We were able to use these residual count rates to estimate the scattered-light correction near strong lines (specifically, H_2 lines arising from the $J = 0$ and $J = 1$ levels), but we were less certain of the scattered-light levels far from these lines, where some of the weaker, moderately high J lines are found (this is discussed further below).

c) *Equivalent Width Measurements*

Smooth lines were drawn through the spectra, and the equivalent widths of the H_2 lines were measured by hand; the data quality did not warrant any more sophisticated technique. The formal uncertainties in the equivalent widths were derived using the algorithm of Jenkins *et al.* (1973), which takes into account photon statistics and the number of pixels required to measure the full width of a line. The additional uncertainty due to poor knowledge of the scattered-light level cannot be formally estimated, but we were able to assess the problem in the many instances where a line appeared twice, in adjacent spectral orders. There was no obvious systematic error due to poor scattered-light correction, so we conclude that on average our technique of using residual count rates at the centers of saturated lines was reasonably accurate. As we explain in § IV, this conclusion is substantiated by the curve-of-growth analysis, which shows reasonable consistency among lines arising from the same rotational state.

Comparison of our equivalent width measurements with those of Spitzer, Cochran, and Hirshfeld (1974), however, revealed a systematic disagreement for the $J = 2$ and $J = 3$ lines, in the sense that our measured values tended to be smaller by some 30%, on average. These lines happen to lie farthest away from the $J = 0$ and $J = 1$ lines on which the scattered-light connections in both the *Copernicus* data and our data were based. Thus, it is reasonable to assume that the discrepancy is due to inadequate correction of scattered light in regions far away from any strongly saturated lines. What is not so easy to determine is for which instrument the corrections was inadequate.

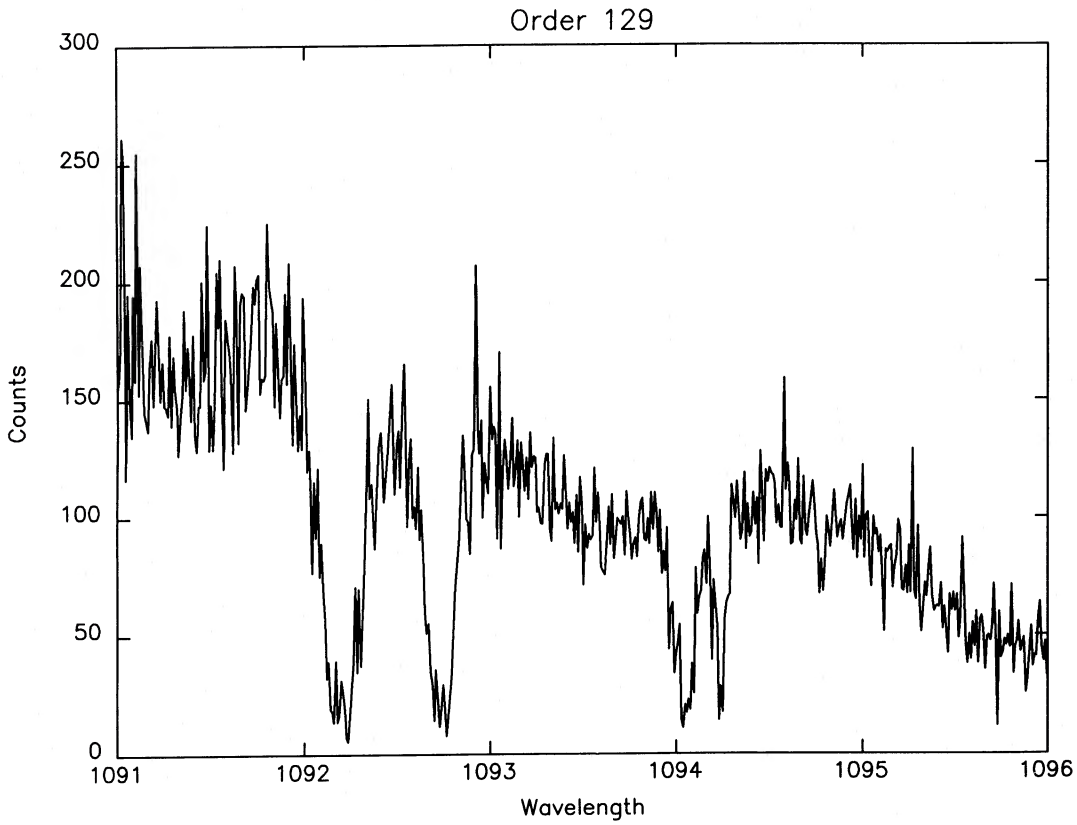

FIG. 1.—Example of data. This shows the (1–0) band at 1092 Å, with a region of continuum (*left*) displaying the extreme noise fluctuations occasionally present in the data. These noisy regions are addressed in the text.

One could argue that our scattered-light correction is more secure, because we were able to obtain interorder measurements in our two-dimensional detector, and because we had available redundant measurements of some lines that appeared in adjacent spectral orders. On the other hand, the scattered-light contribution to our total signal level was somewhat greater than in the *Copernicus* data, leaving more room in our data for significant errors. In any event, we are unable to demonstrate conclusively whether our scattered-light corrections are better or worse than those in the corresponding spectral regions in *Copernicus* data, so we are forced to accept our corrections as they stand. It is noteworthy that the agreement between our data and the *Copernicus* results for regions near strongly saturated lines is quite good.

The measured equivalent widths of H_2 lines in our data are listed in Table 2, along with relevant molecular constants as well as the formal uncertainties. Average values of the equivalent widths, weighted by the continuum level, are given where lines were observed separately in adjacent orders, and in those cases the formal uncertainty reflects the total count rate at the two positions where the line is observed. The line wavelengths and oscillator strengths (f-values) are from Morton and Dinerstein (1976).

d) Velocity Measurements

No attempt was made to establish an accurate prelaunch wavelength scale for the spectrograph; nonetheless, postflight data analysis did allow reasonable limits to be placed on relative velocity positions of H_2 lines arising from the different excited rotational levels. Line centers were measured independently by two of us (T. P. S. and W. E. M.) for 52 separate lines arising from the $J = 0$ to $J = 5$ levels. The position of each line was then calculated using the spectrograph optical configuration and a geometrical ray-trace program. Calculated positions were verified using preflight wavelength data obtained with a hollow cathode platinum lamp equipped with a LiF window. Measured line positions were then fitted to the calculated line positions for each of the 7 echelle orders observed during the flight in order to generate the wavelength shift for individual lines. Wavelength shifts for a fixed value of J but from different echelle orders were then averaged to provide a mean difference (calculated position minus measured position) for all lines arising from the same level.

Figure 2 shows the results of this procedure, where the shift in pixels is plotted as a function of rotational level. Error bars are the formal errors in the mean for each J-value determined from the standard deviation of the pixel differences (calculated minus measured) for the individual lines. There is no evidence for relative velocity shifts for different values of J within ± 1 pixel, corresponding to ± 2.7 km s^{-1}.

We are unfortunately not able to measure line widths with sufficient accuracy to test whether lines arising from high J levels were broader than those from low rotational states. The data were too noisy to allow this to be done.

IV. ABUNDANCE RESULTS

a) Curve-of-Growth Analysis and Total H_2 Abundance

The equivalent width data on lines arising from rotational levels $J = 0$ through $J = 5$ were interpreted using a standard

TABLE 2

H_2 MEASUREMENTS

Line	λ (Å)	f	W (mÅ)	m.e. (mÅ)
$J = 0$ ($g = 1$, $E_J = 0$); log $N = 19.25$ cm^{-2}				
(4–0) $R(0)$.....	1049.366	0.0235	384	9
(3–0) $R(0)$.....	1062.883	0.0182	392	8
(2–0) $R(0)$.....	1077.138	0.0119	343	8
(1–0) $R(0)$.....	1092.194	0.00596	233	8
$J = 1$ ($g = 9$, $E_J = 0.01469$ eV); log $N = 18.99$ cm^{-2}				
(4–0) $R(1)$.....	1049.958	0.0160	235	8
$P(1)$.....	1051.031	0.00749	208	9
(3–0) $R(1)$.....	1063.460	0.0124	215	8
$P(1)$.....	1064.606	0.00584	171	12
(2–0) $R(1)$.....	1077.698	0.00809	168	9
$P(1)$.....	1078.925	0.00385	134	8
(1–0) $R(1)$.....	1092.732	0.00403	156	7
$P(1)$.....	1094.052	0.00193	123	8
$J = 2$ ($g = 5$, $E_J = 0.04394$ eV); log $N = 17.28$ cm^{-2}				
(4–0) $R(2)$.....	1051.497	0.0147	69	11
$P(2)$.....	1053.281	0.00878	57	10
(3–0) $R(2)$.....	1064.995	0.0113	62	7
$P(2)$.....	1066.901	0.00687	67	7
(2–0) $R(2)$.....	1079.226	0.00379	56	9
$P(2)$.....	1081.265	0.00453	72	8
(1–0) $R(2)$.....	1094.244	0.00367	54	8
$P(2)$.....	1096.439	0.00228	69	11
$J = 3$ ($g = 21$, $E_J = 0.08747$ eV); log $N = 17.02$ cm^{-2}				
(4–0) $R(3)$.....	1053.976	0.0142	82	9
$P(3)$.....	1056.469	0.00919	78	7
(3–0) $R(3)$.....	1067.478	0.0109	57	6
$P(3)$.....	1070.142	0.00721	67	8
(2–0) $R(3)$.....	1081.710	0.00713	47	8
$P(3)$.....	1084.559	0.00477	...	...
(1–0) $R(3)$.....	1096.715	0.00354	56	7
$P(3)$.....	.1099.788	0.00240	46	6
$J = 4$ ($g = 9$, $E_J = 0.14491$ eV); log $N = 14.99$ cm^{-2}				
(4–0) $R(4)$.....	1057.379	0.0140	41	9
$P(4)$.....	1060.580	0.00930	18	7
(3–0) $R(4)$.....	1070.898	0.0107	...	...
$P(4)$.....	1074.313	0.00733	50	5
(2–0) $R(4)$.....	1085.144	0.00700	19	9
$P(4)$.....	1088.794	0.00487	...	...
(1–0) $R(4)$.....	1100.165	0.00347	...	...
$P(4)$.....	1104.084	0.00245	...	...
$J = 5$ ($g = 33$, $E_J = 0.21575$ eV); log $N = 1434$ cm^{-2}				
(4–0) $R(5)$.....	1061.697	0.0121	17	10
$P(5)$.....	1065.594	0.00931	16	5
(3–0) $R(5)$.....	1075.244	0.00947	11	6
Total H_2: log $N = 19.44$ cm^{-2}				

curve-of-growth technique (e.g., Spitzer 1978). The result is shown in Figure 3, where lines arising from different J levels are indicated by special symbols. It is seen that the lines from all the observed rotational states fit the same curve (with velocity dispersion parameter $b = 3$ km s^{-1}). Experimentation showed that other, nearby b-values produced fits allowed by the known uncertainties, but that the range of values that could fit all the rotational levels simultaneously was quite narrow. Spitzer, Cochran, and Hirshfeld (1974) found $b = 4.9$ km s^{-1}; our own reanalysis of their data shows that $b = 3$ km s^{-1} provides nearly as good a fit.

The uncertainties in the derived column densities, which are listed in Table 2, are difficult to assess quantitatively. For the $J = 0$ and $J = 1$ lines, the uncertainty is relatively small, for several reasons: (1) these lines are so strong that the photon noise is relatively unimportant; (2) the scattered-light level is most accurately known for them; and (3) they are nearly on the damping portion of the curve, where there is no dependence on the b-value. As it is, we can say confidently that we have not significantly underestimated the column densities for $J = 0$ and $J = 1$, because for larger column densities the equivalent widths would have to be larger than observed. We may have overestimated the column densities, but only if the true b-value is significantly larger than 3 km s^{-1}, contrary to experience with other lines of sight.

For the higher rotational states, the uncertainties on the column densities are probably greater. No doubt the absolute value of the column density for any specific rotational state is uncertain by at least a factor of 2, given all the possible errors in the equivalent width measurements and the ambiguity of choosing the b-value. This latter source of error, however, has less effect on the *relative* column densities of the different rotational states, because the column density will tend to change in the same sense for each J level as the result of a given change in b (so long as it is correct to assume that the same b-value applies to all rotational states).

Our column densities agree quite well with those of Spitzer, Cochran, and Hirshfeld (1974) for $J = 4$ and $J = 5$, but they disagree for $J = 2$ and $J = 3$. Ironically, in these rotational states where our equivalent widths are systematically *smaller*, our column densities are *larger*. This reflects the fact that Spitzer, Cochran, and Hirshfeld adopted a larger b-value than we did. The degree of mismatch between our results and theirs for $J = 2$ and $J = 3$ should serve as a reminder of the general uncertainty of curve-of-growth results for lines in the flat part of the curve.

The total column density of all the observed rotational levels is $N(H_2) = 2.8 \times 10^{19}$ cm^{-2}. This is remarkably (and fortuitously, given our uncertainties) close to the value of 2.6×10^{19} cm^{-2} found by Savage *et al.* (1977), who used a profile-fitting technique to derive the $J = 0$ and $J = 1$ column densities from *Copernicus* data. The good agreement bolsters our claim for fairly good accuracy, at least in the determination of the column densities for $J = 0$ and $J = 1$.

b) *Rotational Excitation*

Since the relative population of the $J = 0$ and $J = 1$ states is thought to be determined by thermal equilibrium with the gas, the ratio of these populations is normally taken as an indicator of the kinetic temperature in the cloud. Using our column densities for $J = 0$ and $J = 1$, along with the statistical weights g given in Table 2, we find (from the Boltzmann excitation equation) a kinetic temperature of 62 K (Savage *et al.* 1977 report $T = 56$ K).

Figure 4 shows the distribution of all observed J levels. The logarithm of the ratio of column density to statistical weight is plotted against the excitation energy, so that, according to the Boltzmann equation, a given rotational temperature will appear as a straight line. We see in the figure that the data are approximately represented by two straight lines, one representing the ratio of $J = 1$ to $J = 0$, whose slope corresponds to the 62 K kinetic temperature just discussed, and another representing levels $J = 2$ through $J = 5$, whose slope corresponds to a rotational temperature of 210 K. This type of pattern of

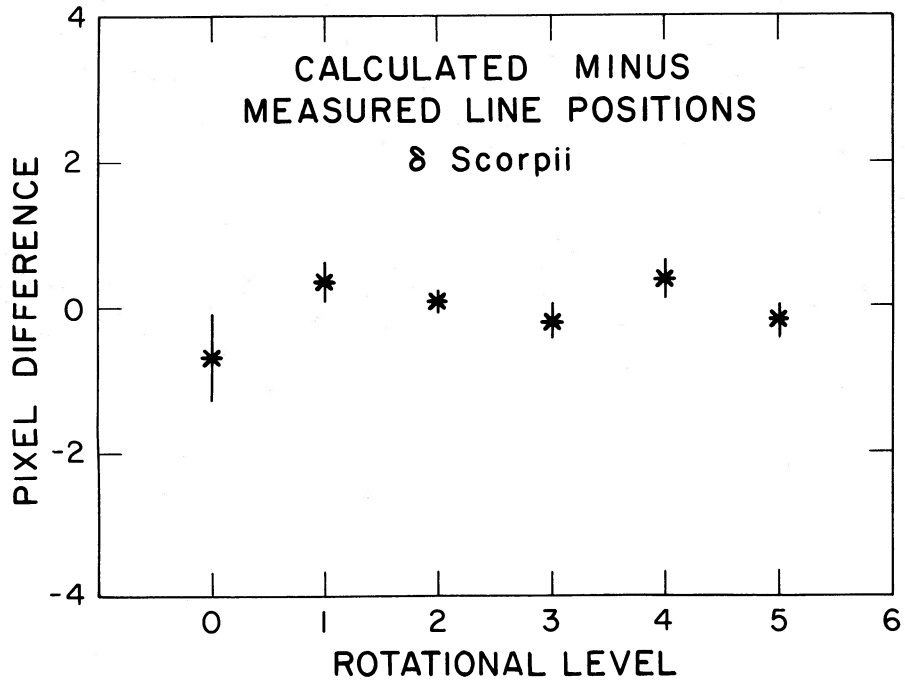

FIG. 2.—Relative wavelength accuracy in the δ Sco data. For each rotational level, measured line positions were compared with those computed from a detailed analysis of the spectrograph optics. This shows that, within ± 1 pixel (that is, ± 2.7 km s^{-1}), the mean velocity of the lines for each rotational level is the same. This shows that, within ± 1 pixel (that is, ± 2.7 km s^{-1}), the mean velocity of the lines for each rotational level is the same. The error bars plotted for each level are ± 1 σ, where σ is the standard deviation from the mean for all the measured lines of that level.

rotational excitation in H_2 is commonly seen (e.g., Spitzer, Cochran, and Hirshfeld 1974, who find an excitation temperature of 317 K for δ Sco), and the excitation of the $J > 2$ levels is attributed to ultraviolet pumping, as explained in § I. The fact that the observed high J levels nearly conform to a straight line in Figure 4 is not physically meaningful, since the relative populations of these levels are not due to a physical temperature.

V. INTERPRETATION

a) Derivation of Physical Conditions

As noted in § I, the excitation of high rotational levels is generally attributed to ultraviolet pumping, with a contribution due to the formation of H_2 molecules in excited states. Jura (1975*a*, *b*) has developed models for the population of the high J levels in H_2, in both the optically thin and the optically thick cases. For δ Sco, the optically thick case is relevant, because the $J = 0$ and $J = 1$ lines are saturated.

From the rate equations for the excitation and de-excitation processes presented by Jura, it is possible to use the observed column densities to derive the radiation field intensity (which governs excitation by ultraviolet pumping) and the formation rate of H_2 molecules.

The population of the $J = 4$ level is most strongly dominated by ultraviolet pumping according to Jura's model, so the column density of this level is probably the best indicator of the radiation field intensity. Using our data with Jura's model, along with the spontaneous emission probability for $J = 4$ to $J = 2$ from Turner, Kirby-Docken, and Dalgarno (1977), we find that the rate of photoexcitation in the Lyman and Werner bands is $\beta_0 = 4.9 \times 10^{-13}$ s^{-1} (we get a value of 1.0×10^{-12} s^{-1} from the observed population of the $J = 5$ level, for which ultraviolet pumping is relatively unimportant, so we adopt the value from $J = 4$).

To convert the estimated rate of photoexcitation of H_2 molecules into an interstellar radiation field intensity in conventional units requires summing the total number of excitations in the line of sight, as indicated by the total equivalent width of all absorption lines from $J = 0$ in the Lyman and Werner bands, and setting this equal to the total rate of radiative de-excitations from $J = 4$, allowing for the fraction of the latter that go into states other than $J = 0$. The procedure is described in Wright and Morton (1979). The result of doing this for δ Sco is that the average ultraviolet radiation field intensity (in the interval 912–1100 Å) is $U = 8.9 \times 10^{-29}$ ergs cm^{-3} Hz^{-1}. According to Witt and Johnson (1973), the average value in this wavelength interval in the vicinity of the Sun is 1.5×10^{-29} ergs cm^{-3} Hz^{-1}.

We conclude that the radiation field where the molecular hydrogen exists in the line of sight toward δ Sco is roughly 6 times the average interstellar value. This refers to the outer edge of the cloud, because the ultraviolet pumping takes place only there; the inner regions of a diffuse cloud with optically thick H_2 are strongly self-shielded in the $J = 0$ and $J = 1$ lines of the Lyman and Werner bands.

The conclusion that the ultraviolet radiation field in the line of sight toward δ Sco is relatively intense compared to the average interstellar value is consistent with earlier suggestions that the ρ Oph region in general has a high radiation field intensity. Snow (1983*a*) analyzed literature data on σ Sco, finding from the rotational excitation of H_2 in that line of sight a value even higher than we find here for δ Sco. The high intensity of radiation in such reddened lines of sight is prob-

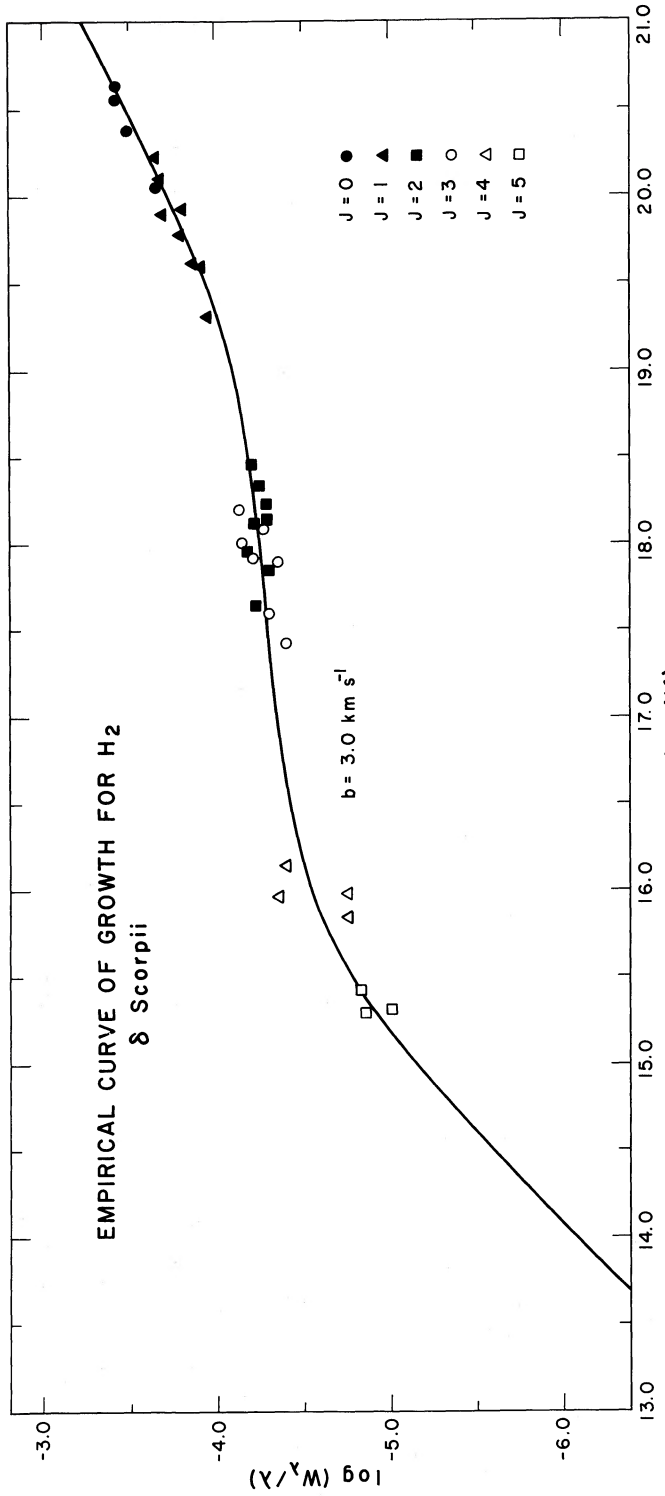

FIG. 3.—Curve of growth for H_2 lines toward δ Sco. The equivalent widths for rotational levels $J = 0$ through $J = 5$ fit a theoretical curve with velocity dispersion parameter $b = 3$ km s^{-1}.

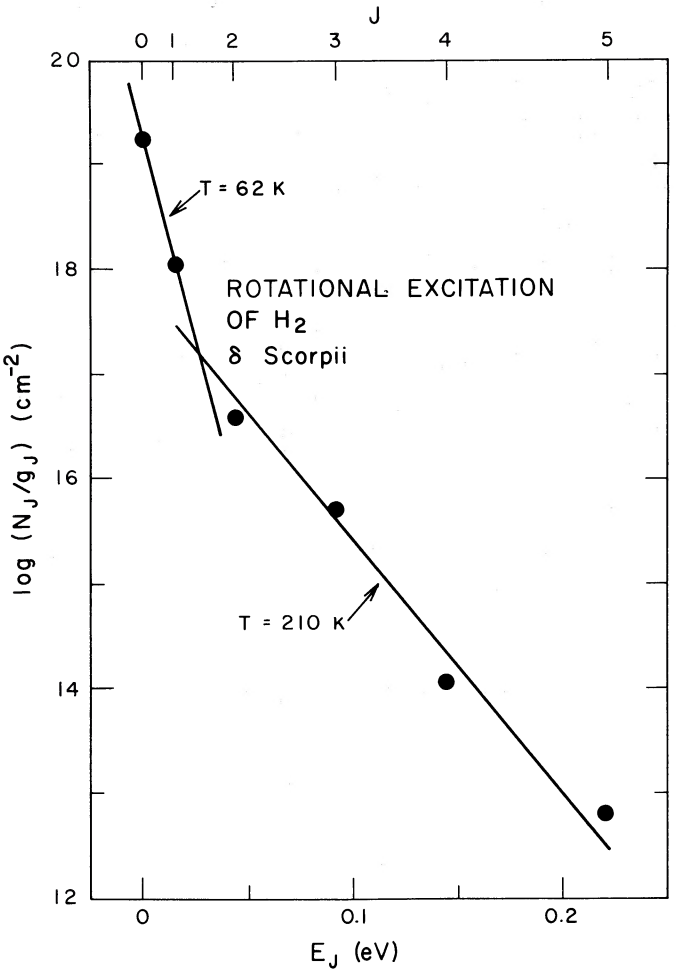

FIG. 4.—Rotational excitation in H_2 toward δ Sco. The $J = 0$ and $J = 1$ populations are consistent with a kinetic temperature of 62 K, while the higher rotational states roughly fit an excitation temperature of 210 K.

ably attributable to forward-scattering grains (Witt *et al.* 1982; Flannery, Roberge, and Rybicki 1980).

b) Cloud Density and H_2 Formation Rate

From Jura's model for rotational excitation in H_2 it is also possible to estimate the rate of H_2 formation, since this contributes to the rotational excitation. The parameter actually derived from the analysis is the product Rn, where R is the formation rate of H_2 molecules in units of $cm^3\ s^{-1}$ and n is the total volume density of hydrogen nuclei. From our analysis of the δ Sco data, we find $Rn = 1.6 \times 10^{-15}\ s^{-1}$ from the $J = 4$ population, and $Rn = 1.5 \times 10^{-15}\ s^{-1}$ from the $J = 5$ population.

Having derived the product Rn, we now seek to find the values for the two separately. Jura (1974) argued for a general value of $R \approx 10^{-17}\ cm^3\ s^{-1}$, which, if adopted for δ Sco, leads to an estimate for the hydrogen density of $n \approx 150\ cm^{-3}$. This value, combined with our temperature estimate of 62 K, appears consistent with the value of the pressure nT derived from C I excitation measurements by Jenkins and Shaya (1979), but their results are not very restrictive for this star.

Other data may indicate that R is unusually low for the ρ Oph region. In the hydrogen survey of Bohlin, Savage, and Drake (1978), it was found that the molecular fraction in the ρ Oph region tends to be significantly lower than in other diffuse clouds of comparable reddening. Other evidence (Jura 1980) indicates that the extinction per unit mass of grains is unusually low in this region, leading to the suggestion (Jura 1980) that grains there have coagulated. Snow (1983*b*) pointed out that the coagulation of grains would reduce the total surface area available for H_2 formation, and showed that the reduction in surface area expected from Jura's analysis of the extinction is consistent with the amount by which the formation rate of H_2 would have to be reduced to explain the low molecular fraction of hydrogen. The conclusion reached by Snow was that the H_2 formation rate may be reduced by a factor of 2–3.

Thus, the value of R appropriate for δ Sco should perhaps be in the range of $(3–5) \times 10^{-18}\ cm^3\ s^{-1}$. This, combined with our value of $Rn = 1.5 \times 10^{-15}\ s^{-1}$, leads to an estimated hydrogen density of $n = 300–500\ cm^{-3}$. This yields a product nT that is still easily consistent with the C I excitation analysis of Jenkins and Shaya (1979). These values are typical for relatively dense diffuse clouds. We will soon be able to estimate n for the δ Sco line of sight from ionization equilibrium, as part of a current program to analyze archival *Copernicus* data (Snow, Allen, and Jenkins 1987).

c) Rotational Line Velocities and Circumstellar Bubbles

As noted in an earlier section, one of the goals of this study was to take advantage of the high spectral resolution to search for any systematic velocity separation between lines arising from different rotational levels. The basis for this was the earlier *Copernicus* work of Spitzer and Morton (1976), which suggested that the high-J lines arise in material being expelled from the background O or B star.

Our analysis of the line velocities indicates that any systematic *relative* shifts of more than 1 pixel would have been detected, yet no such shifts were found among the lines from levels higher than $J = 2$. Hence we conclude that in the H_2 observed toward δ Sco, the rotationally excited molecules all have the same radial velocity to within $\pm 3\ km\ s^{-1}$. Because of the width and saturation of the low-excitation lines, we cannot determine whether they arise at the same velocity. As noted earlier, we also were unable to determined whether the high-J lines were systematically broadened with respect to lines from lower levels.

Our finding appears to indicate that the H_2 toward δ Sco does not have a significant component arising in a circumstellar shell or bubble. Because the star itself does not have a very strong wind, however, this says little about the Spitzer and Morton results, or about the general theoretical picture of circumstellar bubbles.

VI. SUMMARY

The data described in this study are believed to be the highest resolution observations of interstellar H_2 absorption lines yet published. The analysis has led to column density measurements for hydrogen molecules in rotational levels $J = 0$ through $J = 5$, but because of signal-to-noise limitations a detailed study of line profiles was prohibited. Nevertheless, we have been able to determine the kinetic temperature of the cloud containing the observed H_2, and we have shown that there is little or no systematic velocity separation among the excited rotational levels.

In the future we hope to carry out similar analyses with better signal-to-noise ratios, and we will select stars known to have strong winds, so that the circumstellar bubble implications can be better explored.

This research has been supported by National Aeronautics and Space Administration grant NSG-5303 to the University of Colorado. We thank E. B. Jenkins for his thoughtful and detailed comments on the manuscript.

REFERENCES

Black, J. H., and Dalgarno, A. 1976, *Ap. J.*, **203**, 132.
Blades, C., Wynn-Jones, I., and Wayte, R. C. 1980, *M.N.R.A.S.*, **193**, 849.
Bohlin, R. C., Savage, B. D., and Drake, J. F. 1978, *Ap. J.*, **224**, 132.
Carrasco, L., Strom, S. E., and Strom, K. M. 1973, *Ap. J.*, **182**, 95.
Carruthers, G. 1970, *Ap. J. (Letters)*, **161**, L81.
Castor, J. I., McCray, R. A., and Weaver, R. 1975, *Ap. J. (Letters)*, **200**, L107.
Flannery, B. P., Roberge, W., and Rybicki, G. B. 1980, *Ap. J.*, **236**, 598.
Hobbs, L. M. 1978, *Ap. J. Suppl.*, **38**, 129.
Jenkins, E. B. 1973, *Ap. J.*, **181**, 761.
Jenkins, E. B., Drake, J. F., Morton, D. C., Rogerson, J. B., Spitzer, L., and York, D. G. 1973, *Ap. J. (Letters)*, **181**, L122.
Jenkins, E. B., and Shaya, E. J. 1979, *Ap. J.*, **231**, 55.
Jura, M. 1974, *Ap. J.*, **191**, 375.
———. 1975*a*, *Ap. J.*, **197**, 575.
———. 1975*b*, *Ap. J.*, **197**, 581.
———. 1980, *Ap. J.*, **235**, 63.
Meyers, K. A., Snow, T. P., Federman, S. R., and Breger, M. 1985, *Ap. J.*, **288**, 148.
Morton, D. C., and Dinerstein, H. 1976, *Ap. J.*, **204**, 1.
Morton, D. C., Drake, J. F., Jenkins, E. B., Rogerson, J. B., Spitzer, L., and York, D. G. 1973, *Ap. J. (Letters)*, **181**, L103.
Savage, B. D., Bohlin, R. C., Drake, J. F., and Budich, W. 1977, *Ap. J.*, **216**, 291.
Shull, J. M., and Beckwith, S. 1983, *Ann. Rev. Astr. Ap.*, **20**, 163.
Snow, T. P. 1981, *Ap. J.*, **251**, 139.
———. 1983*a*, *Ap. J.*, **266**, 576.
———. 1983*b*, *Ap. J. (Letters)*, **269**, L57.
Snow, T. P., Allen, M. M., and Jenkins, E. B. 1987, in preparation.
Snow, T. P., and Jenkins, E. B. 1980, *Ap. J.*, **241**, 161.
Snow, T. P., and Morton, D. C. 1976, *Ap. J. Suppl.*, **32**, 429.
Spitzer, L. 1978,
Spitzer, L., Cochran, W. D., and Hirshfeld, A. 1974, *Ap. J. Suppl.*, **28**, 373.
Spitzer, L., and Jenkins, E. B. 1975, *Ann. Rev. Astr. Ap.*, **13**, 133.
Spitzer, L., and Morton, W. A. 1976, *Ap. J.*, **204**, 731.
Spitzer, L., and Zweibel, E. G. 1974, *Ap. J. (Letters)*, **191**, L127.
Timothy, J. G., and Bybee, R. L. 1981, *Proc. Soc. Photo-Opt. Instr. Eng.*, **265**, 93.
Turner, J., Kirby-Docken, K., and Dalgarno, A. 1977, *Ap. J. Suppl.*, **35**, 281.
Weaver, R., McCray, R., Castor, J., Shapiro, P., and Moore, R. 1977, *Ap. J.*, **220**, 742.
Witt, A. N., and Johnson, M. W. 1973, *Ap. J.*, **181**, 363.
Witt, A. N., Walker, G. A. H., Bohlin, R. C., and Stecher, T. P. 1982, *Ap. J.*, **261**, 492.
Wright, E. L., and Morton, D. C. 1979, *Ap. J.*, **227**, 483.

WILLIAM E. McCLINTOCK: Laboratory for Atmospheric and Space Physics, University of Colorado, Campus Box 392, Boulder, CO 80309

THEODORE P. SNOW: Center for Astrophysics and Space Astronomy, University of Colorado, Campus Box 391, Boulder, CO 80309

STEPHEN A. VOELS: Joint Institute for Laboratory Astrophysics, University of Colorado, Campus Box 440, Boulder, CO 80309